Accepted for publication in **Vietnam Journal of Mathematics**, August 2018

An optimization framework for the computation of time-periodic solutions of partial differential equations

Thomas Richter* Winnifried Wollner†

Within this article, we analyze an optimization based framework for the calculation of time periodic solutions of linear partial differential equations. To this end, we introduce a suitable set of shooting variables (initial values), and a cost functional whose minimizers correspond to the desired periodic states. We show that if the linear partial differential equations satisfies a smoothing property, a unique minimizer exists. The approach is complemented by numerical examples.

1 Introduction

Many dynamical systems admit a solution with a periodic state $u(t) = u(t+T)$ where T is the length of one period. Such problems appear in fluid-dynamics in the regime of moderate Reynolds numbers, either by an oscillatory forcing of known periodicity [16, 10] or by the von Kármán vortex street arising in the flow around an obstacle [9]. Other examples are found in chemical process engineering, where so called cyclic steady states are the desired operation modes in moving bed processes [26] for chromatographic separation [18]. In various chemical applications, periodic solutions are more efficient than stationary outputs [33]. In some of these examples the periodicity is known and enforced by means of the problem data (like the frequency of moving bed devices), other configurations like the flow around an obstacle yield a certain periodicity by the inner dynamics of the coupling.

The necessity to compute cyclic solutions also arises in temporal multiscale methods, where the problem features temporal microscales, that are oscillating at a high frequency. A typical example is found in damage mechanics, e.g., the deterioration of a mechanical structure (bridge or house) that will suffer slow decay and accumulation of damage over a very long period (time scale t), caused by high frequent oscillatory impulses (time scale $\tau \ll t$). Another example is found in the fluid dynamical forces (the oscillating wall shear stress) of the pulsating blood flow (time scale τ) on vessel walls that can cause damages and long time growth of stenosis [30] (time scale $t \gg \tau$). Often it is not possible to resolve the temporal microscale while performing long-time simulations and stationary simplifications are considered [31]. Temporal multiscale techniques for such long-term problems with

*Universität Magdeburg, Institut für Analysis und Numerik, Universittsplatz 2, 39106 Magdeburg, Germany, thomas.richter@ovgu.de

†TU Darmstadt, Fachereich Mathematik, Dolivostr. 15, 64293 Darmstadt, Germany, wollner@mathematik.tu-darmstadt.de

short-term influences can be based on the solution of effective long-term equations that are obtained by averaging and that depend on the input of periodic short-term problems [6, 7]. Such an approach has been undertaken in [8] for the plaque formation problem. It has however proven to be essential to determine the periodic microscale problems up to low tolerances.

The computation of periodic states by brute-force forward simulation may take an excessive number of cycles to be run. Given a periodic forcing the convergence to the cyclic state will mainly depend on an interplay of energy conservation and smoothing properties of the underlying system of equations. In [21] a scheme is developed to approximate periodic solutions by a monotone iteration scheme. In literature several approaches are discussed for accelerating this solution procedure. [25] showed that under certain conditions an undamped Newton scheme converges towards a periodic solution. In [15] the authors formulate a Newton scheme for the periodicity error $F(q) := u(t+T)-q \stackrel{!}{=} 0$ where $u(t) = q$ is the initial value. This results in a technique similar to the shooting method that requires the solution of a matrix-valued sensitivity system. The authors of [22] propose a global space-time discretization for a direct computation of the cyclic state, formulating the periodic equation as a boundary value problem in space and time. Both approaches have to face the challenge of dimensionality: the shooting approach requires to compute M steps of a matrix valued sensitivity system of size N^2 (where N is the number of spatial unknowns, M the number of time steps), the global space-time approach results in a coupled system of size $M \times N$. Both approaches are difficult to extend to 2d or 3d problems involving partial differential equations requiring high spatial resolution with $N \gg 1\,000\,000$. Shooting type methods can be accelerated by employing matrix free Newton-Krylov approaches as demonstrated by Wilkening et al. [12, 32]. Instead of assembling the high dimensional and possibly dense Jacobian, each matrix vector multiplication of the Jacobian is computed as one tangent problem. Given a sufficiently small tolerance in the inner Krylov subspace methods the authors reach quadratic convergence of the shooting method. The authors use time and space discretization techniques of high order. The authors of [13] consider optimization problems that are subject to periodic solutions of a parabolic problem. Preconditioned Newton-Picard iterations are developed to accelerate the finding of periodic states.

In [18] the authors present a cascadic multilevel method to accelerate the forward simulation by using approximated systems in space and time. Although this approach might suffer from long transition times its extension to PDEs with high dimension of the spatial problem is straightforward.

In this contribution, we will formulate the cyclic steady state problem as a constrained minimization problem: we search for initial data $q \in Q$ such that

$$\|u_q(T) - q\|_Q^2 \to 0,$$

where $u_q(t)$ is given as the solution of the dynamical system $u_q'(t) = f(t, u_q(t))$ with $u_q(0) = q$. A similar approach is considered in [1] for the computation of time periodic solutions to the Benjamin-Ono equation using high order discretization schemes. The approach corresponds to single-shooting for the boundary-value problem in time, and can easily be extended to multiple-shooting intervals, cf., [5].

The outline of the paper is as follows. In Section 2, we will provide an abstract framework for the above minimization problem, for the determination of the periodic states. In particular, we show that for equations satisfying a smoothing property the minimization of the above problem is possible without any further regularization terms in the functional, and that the unique minimizer is indeed a periodic solution. We will show in Section 3, that the requirements of the abstract setting are met by a strongly damped wave equation. In the context of time periodic problems hyperbolic equations are often found, e.g., in damage mechanics where elastic structure are excited by periodic forcing. Quick identification of periodic solutions is important as small changes in material parameters can result in completely different resonance regimes. In Section 4, we will discuss how the resulting

minimization problem can be solved numerically. Besides the description of the gradient method and the Newton scheme for approximating the minimization problem introduced in Section 2, we shortly describe the discretization in space and time. Section 5 discusses two numerical test cases, the linear strongly damped wave equation and a nonlinear problem where an additional nonlinear coupling term is introduced. We finally provide some conclusions in Section 6.

2 Abstract Setting

In order to analyze the method under consideration, we first provide an abstract form for the control to state mapping. To this end, let $\Omega \subset \mathbb{R}^d$, with $d \in \mathbb{N}$, be a, sufficiently smooth, domain and let $I = (0,T)$ be a given time interval. Let Q be a Hilbert-space of admissible initial values, i.e., Q contains functions $q\colon \Omega \to \mathbb{R}^c$, $c \in \mathbb{N}$, of a certain regularity. Further, let W be another Hilbert-space of functions $u\colon I \times \Omega \to \mathbb{R}^c$ satisfying $W \subset C(\overline{I}, Q) \cap C(\overline{I}, L^2(\Omega))$.

We are concerned with periodic solutions, $u(T) = u(0)$, to the evolutionary PDE

$$\begin{aligned} \partial_t u(t,x) + \mathcal{A}u(t,x) &= f(t,x) && \text{in } I \times \Omega, \\ u(0) &= q && \text{in } \Omega, \end{aligned}$$

together with appropriate boundary values on $I \times \partial\Omega$.

For convenience, we define a corresponding variational form. Let $(\cdot,\cdot)_Q$ and $\|\cdot\|_Q$ be the scalar product and norm on Q, $((\cdot,\cdot))$ and $|||\cdot|||$ be the scalar product and norm on $L^2(I, L^2(\Omega))$ and $A\colon W \times W \to \mathbb{R}$ be a given continuous bilinear mapping. Then given an initial-value $q \in Q$, we associate a state $u = u_q \in W$ as a solution to

$$((\partial_t u, \phi)) + A(u,\phi) + (u(0), \phi(0))_Q = ((f,\phi)) + (q, \phi(0))_Q \qquad \forall \phi \in W \tag{1}$$

where $f \in L^2(I, L^2(\Omega))$ is a given right-hand side. In order for this mapping to be well defined, we assume the following

Assumption 1 *For any given $q \in Q$ there exists a unique solution u_q with $u_q(0) = q$ of (1). Further, this solution satisfies the stability estimate*

$$\|u(T)\|_Q \le c(\|q\|_Q + c_F)$$

with a constant c_F depending on the chosen data f, where $c_0 = 0$.

Example 2 *The most simple example for the above setting is the heat equation*

$$\begin{aligned} \partial_t u(t,x) - \Delta u(t,x) &= f(t,x) && \text{in } I \times \Omega, \\ u(0,x) &= q(x) && \text{in } \Omega, \\ u(t,x) &= 0 && \text{on } \partial\Omega. \end{aligned}$$

Here $Q = L^2(\Omega)$ and $W = W(0,T) = \{v \in L^2(I, H_0^1) \,|\, \partial_t v \in L^2(I, (H_0^1(\Omega))^*)\}$ and the weak form of the initial value problem is given by

$$((\partial_t u, \phi)) + ((\nabla u, \nabla \phi)) + (u(0), \phi(0)) = ((f,\phi)) + (q, \phi(0))$$

for any $\phi \in W$, where $(\cdot,\cdot)$ denotes the $L^2(\Omega) = Q$ scalar product - here the H_0^1-$(H_0^1)^*$ duality pairing is identified with the L^2-scalar product. It is then well-known that Assumption 1 is satisfied, see, e.g., [29, Chapter 26].

Example 3 *The same setting can be transferred to the incompressible Stokes equations considering the function space $Q = L^2(\Omega)^d$, where d is the spatial dimension. Further, we can extend Assumption 1 to the nonlinear Navier-Stokes equations. Assuming the existence of a solution on $I = [0, T]$ and given homogeneous Dirichlet values on the complete boundary Ω (required for dealing with the nonlinearity $((u \cdot \nabla u, \phi))$), the assumption holds for $Q = L^2(\Omega)^d$. The major difficulty in handling the Navier-Stokes equations however is the question of existence (and uniqueness) of periodic in time solutions which is only known for small Reynolds numbers [10].*

Based upon the well-posed forward problem, we can now formulate an optimization problem for the time-periodic setting.

$$\begin{aligned} \min_{q \in Q, u \in W} \ & \frac{1}{2}\|q - u(T)\|_Q^2 \\ & \text{s.t. } u,\ q \text{ solve (1).} \end{aligned} \tag{2}$$

It is clear, that the minimal value of (2) is zero if and only if the corresponding minimizer q, u satisfy $q = u(0) = u(T)$.

When considering this problem, the difficulty lies in the fact, that while $\|\cdot\|_Q^2$ is uniformly convex the composed mapping $(q, u) \mapsto \|q - u(T)\|_Q^2$ is not. Consequently, a small trick is needed to assert that indeed a minimum exists.

Theorem 4 *Let Assumption 1 be satisfied with $c < 1$. Then Problem (2) has exactly one minimizer.*

Proof: Clearly, the functional is convex, and thus any local minimizer is global. We will now see, that the functional is strictly convex. This asserts that there is at most one minimizer of (2).

To this end, let $q, \tilde{q} \in Q$ be arbitrary with corresponding states $u, \tilde{u}$. Then for any $\lambda \in (0, 1)$ it is

$$\begin{aligned} \|\lambda(q - u(T)) + (1 - \lambda)(\tilde{q} - \tilde{u}(T))\|_Q^2 = \lambda\|q - u(T)\|_Q^2 + (1 - \lambda)\|\tilde{q} - \tilde{u}(T)\|_Q^2 \\ - \lambda(1 - \lambda)\|q - u(T) - \tilde{q} + \tilde{u}(T)\|_Q^2. \end{aligned}$$

Clearly, if $q - u(T) - \tilde{q} + \tilde{u}(T) \neq 0$ a strict inequality, and thus strict convexity, holds. Assume, to the contrary that the above would be zero, then

$$q - \tilde{q} = u(T) - \tilde{u}(T)$$

and moreover it holds

$$\begin{aligned} \partial_t(u - \tilde{u}) + \mathcal{A}(u - \tilde{u}) &= 0 && \text{in } I \times \Omega, \\ (u - \tilde{u})(0) &= q - \tilde{q} && \text{in } \Omega. \end{aligned}$$

By the stability estimate of Assumption 1, we have

$$\|(u - \tilde{u})(T)\|_Q \leq c\|q - \tilde{q}\|_Q < \|q - \tilde{q}\|_Q$$

since $c < 1$ contradicting the equality $(u - \tilde{u})(T) = q - \tilde{q}$. Thus the functional is strictly convex, and at most one minimizer exists.

To show existence of a minimizer, we abbreviate $j(q, u) = \frac{1}{2}\|q - u(T)\|_Q^2$, and see immediately that $0 \leq j(q, u)$ and hence there exists $\bar{j} = \inf_{q,u} j(q, u)$. Consequently, there exists a minimizing sequence

(q_k, u_k) with $u_k = u_{q_k}$. With the same calculation as above (and $\lambda = \frac{1}{2}$), we get the following for the minimizing sequence:

$$\begin{aligned}
\frac{1}{4}\|q_l - q_m + u_m(T) - u_l(T)\|_Q^2 &= \frac{1}{2}\|q_l - u_l(T)\|_Q^2 + \frac{1}{2}\|q_m - u_m(T)\|_Q^2 \\
&\quad - \|\frac{1}{2}(q_l - u_l(T)) + \frac{1}{2}(q_m - u_m(T))\|_Q^2 \\
&= j(q_l, u_l) + j(q_m, u_m) \\
&\quad - 2\frac{1}{2}\|\frac{1}{2}(q_l + q_m) - \frac{1}{2}(u_l + u_m)\|_Q^2 \\
&= j(q_l, u_l) + j(q_m, u_m) \\
&\quad - 2j(\frac{1}{2}(q_l + q_m), \frac{1}{2}(u_l + u_m)) \\
&\leq j(q_l, u_l) + j(q_m, u_m) - 2\bar{j} \\
&\to 0 \qquad (l, m \to \infty).
\end{aligned}$$

Now, by the reverse triangle inequality

$$\big|\|q_l - q_m\|_Q - \|u_l(T) - u_m(T)\|_Q\big| \leq \|q_l - q_m + u_m(T) - u_l(T)\|_Q \to 0.$$

By the stability estimate $\|u_m(T) - u_l(T)\|_Q \leq c\|q_l - q_m\|_Q$, we see that

$$\begin{aligned}
0 &\leq (1-c)\|q_l - q_m\|_Q \\
&\leq (1-c)\|q_l - q_m\|_Q + c\|q_l - q_m\|_Q - \|u_m(T) - u_l(T)\|_Q \\
&= \|q_l - q_m\|_Q - \|u_m(T) - u_l(T)\|_Q \\
&= \big|\|q_l - q_m\|_Q - \|u_m(T) - u_l(T)\|_Q\big|.
\end{aligned}$$

Hence the minimizing sequence q_k is a Cauchy-sequence and the assertion follows.

Remark 5 *The assumption $c < 1$ made in the statement of the theorem is only needed for the case $f \equiv 0$. Here it is a reasonable assumption. For example, if considering the heat equation*

$$((\partial_t u, \phi)) + ((\nabla u, \nabla \phi)) + (u(0), \phi(0)) = (q, \phi(0)),$$

one can test with $\phi = tu$ to get the estimate

$$T \int_\Omega |u(T,x)|^2 \,\mathrm{d}x \leq \int_I \int_\Omega |u(t,x)|^2 dx.$$

Together with a stability estimate for $\int_I \int_\Omega |u(t,x)|^2 dx$ one obtains the result

$$\int_\Omega |u(T,x)|^2 \,\mathrm{d}x \leq \frac{c}{T}\|q\|^2$$

showing that $c < 1$ is reasonable once T is sufficiently large.

Finally, we remark, that if the analog of Assumption 1 holds for the adjoint problem

$$\begin{aligned}
-\partial_t z(t,x) + \mathcal{A}^* z(t,x) &= 0 && \text{in } I \times \Omega, \\
z(T) &= u(T) - q && \text{in } \Omega,
\end{aligned}$$

i.e., the estimate

$$\|z(0)\|_Q \le c\|u(T) - q\|_Q$$

holds for some $c < 1$, then the unique minimize of (2) is indeed a periodic solution. To see this, we note, that Lagrange calculus asserts that for the minimizer $\bar{q}, \bar{u}$ of (2) there is a corresponding adjoint $\bar{z}$ solving the above adjoint problem with data $\bar{u}(T) - \bar{q}$. With this, standard calculus, see, e.g., [27], gives the first order necessary optimality condition

$$\bar{u}(T) - \bar{q} + \bar{z}(0) = 0.$$

Assuming that the minimizer is not periodic, i.e., $\bar{u}(T) - \bar{q} \neq 0$, the stability estimate with $c < 1$ asserts,

$$\|\bar{z}\|_Q \le c\|\bar{u}(T) - \bar{q}\|_Q < \|\bar{u}(T) - \bar{q}\|_Q$$

contradicting the optimality condition.

3 The damped wave equation

As a typical example of an equation with oscillatory behavior, we discuss the strongly damped wave equation.

$$\begin{aligned} \partial_t v - \mu\Delta u - \lambda\Delta v &= f && \text{in } I\times\Omega,\\ \partial_t u - v &= 0 && \text{in } I\times\Omega,\\ u(0) &= q_u && \text{in } \Omega,\\ v(0) &= q_v && \text{in } \Omega,\\ u(t,x) &= 0 && \text{on } I\times\partial\Omega \end{aligned} \tag{3}$$

where $I = (0,T)$ and $\Omega \subset \mathbb{R}^d$ is a domain with sufficiently smooth boundary, $f \in L^2(I, H^{-1}(\Omega))$, and $\mu, \lambda > 0$. It is well known, that for any initial data $q_v \in L^2(\Omega)$ and $q_u \in H_0^1$ this equation admits a solution $v \in C(\overline{I}, L^2(\Omega)) \cap L^2(I, H_0^1(\Omega))$ and $u \in C(\overline{I}, H_0^1(\Omega))$, see, e.g., [28, 2] also allowing for a potential nonlinearity in the equation.

We will now see, that indeed Assumption 1 is satisfied on the space

$$Q = \{(q_v, q_u) \in L^2(\Omega) \times H_0^1(\Omega)\}$$

with corresponding norm

$$\|q\|_Q^2 = \|q_v\|^2 + \|\nabla q_u\|^2. \tag{4}$$

Theorem 6 *There exists a constant $c > 0$ such that the unique solution (u, v) of (3) with $f \equiv 0$ satisfies the estimate*

$$\|(v(T), u(T))\|_Q^2 \le \frac{c}{T}\|(v(0), u(0))\|_Q^2,$$

where $c > 0$ depends on the domain Ω and on the parameters μ, λ, e.g., $c = \mathcal{O}(\lambda + \lambda^{-1})$.

Proof: To see the assertion, we multiply the first equation in (3) with a function $\phi \in L^2(I, H_0^1(\Omega))$ and integrate over $I \times \Omega$ to get

$$((\partial_t v, \phi)) + \mu((\nabla u, \nabla\phi)) + \lambda((\nabla v, \nabla\phi)) = 0. \tag{5}$$

Now, selecting $\phi = v = \partial_t u$, we obtain

$$\begin{aligned} 0 &= ((\partial_t v, v)) + \mu((\nabla u, \nabla v)) + \lambda((\nabla v, \nabla v)) \\ &= \frac{1}{2}\|v(T)\|^2 - \frac{1}{2}\|v(0)\|^2 + \frac{\mu}{2}\|\nabla u(T)\|^2 - \frac{\mu}{2}\|\nabla u(0)\|^2 + \lambda|||\nabla v|||^2. \end{aligned}$$

Utilizing Poincaré's inequality this shows

$$\begin{aligned} \|(v(T), u(T))\|_Q^2 + \lambda|||\nabla v|||^2 &\le c\|(v(0), u(0))\|_Q^2, \\ \lambda|||v|||^2 &\le c\|(v(0), u(0))\|_Q^2 \end{aligned}$$

with a constant c depending on μ. Now, testing (5) with $\phi = u$, we assert

$$\begin{aligned} 0 &= ((\partial_t v, u)) + \mu((\nabla u, \nabla u)) + \lambda((\nabla v, \nabla u)) \\ &= -((v, \partial_t u)) + (v(T), u(T)) - (v(0), u(0)) + \mu|||\nabla u|||^2 \\ &\quad + \frac{\lambda}{2}\|\nabla u(T)\|^2 - \frac{\lambda}{2}\|\nabla u(0)\|^2. \end{aligned}$$

Together with the estimate for $((v, \partial_t u)) = |||v|||^2$ and $\|(v(T), u(T))\|_Q^2$, we assert

$$\mu|||\nabla u|||^2 + \frac{\lambda}{2}\|\nabla u(T)\|^2 \le c(1 + \lambda + \lambda^{-1})\|(v(0), u(0))\|_Q^2.$$

Finally, we test with $\phi = tv$ and obtain

$$\begin{aligned} 0 &= ((\partial_t v, tv)) + \mu((\nabla u, t\nabla v)) + \lambda((\nabla v, t\nabla v)) \\ &= \frac{T}{2}\|v(T)\|^2 - \frac{1}{2}|||v|||^2 + \frac{T\mu}{2}\|\nabla u(T)\|^2 - \frac{\mu}{2}|||\nabla u|||^2 + \lambda|||t^{1/2}\nabla v|||^2. \end{aligned}$$

Together with the estimates for $|||v|||$ and $|||\nabla u|||$ this shows the assertion.

For the following numerical treatment, we can define a weak form for the solution of (3). To this end, let $U = (v, u)$, $q = (q_v, q_u)$, $\Phi := (\phi, \psi)$ and define

$$\begin{aligned} B(U, \Phi) &= ((\partial_t U, \Phi)) + ((\mathcal{A}U, \Phi)) \\ &= ((\partial_t v, \phi)) + \mu((\nabla u, \nabla \phi)) + \lambda((\nabla v, \nabla \phi)) \\ &\quad + ((\partial_t u - v, \psi)) + (v(0), \phi(0)) + (u(0), \psi(0)), \\ F(q; \Phi) &= ((f, \phi)) + (q_v, \phi(0)) + (q_u, \psi(0)) \end{aligned} \tag{6}$$

where, again, $((\cdot, \cdot))$ is the space-time integral. Then the solution U of (3) solves the problem

$$B(U, \Phi) = F(q; \Phi) \quad \forall \Phi \in W := C(\overline{I}, H_0^1(\Omega)) \times C(\overline{I}, L^2(\Omega)).$$

4 Solving the Optimization Problem

We refer to the setting introduced in Section 2. Let $u \in W$ be the solution on $I = [0, T]$ given by the variational formulation

$$B(U, \Phi) = F(q; \Phi) \qquad \forall \Phi \in W, \tag{7}$$

that has been introduced in (6). We aim to find $U(0) = q \in Q$ that minimizes

$$J(q; U(T)) := \min_{q \in Q, U \in W} \frac{1}{2}\|q - U(T)\|_Q^2,$$

such that $U = U_q$ solves (7). It is now straightforward to derive first order necessary optimality conditions, cf., [17, 27, 14]. In order to briefly write the resulting system, we introduce the Lagrangian $L : W \times W \times Q \to \mathbb{R}$ by

$$L(U, Z, q) = J(q; U(T)) + F(q, Z) - B(U, Z).$$

Differentiating the Lagrangian with respect to Z, U, and q gives the optimality system

$$\begin{aligned} B(U, \Phi) &= F(q; \Phi), \\ B(\Phi, Z) &= J'_U(q; U(T))(\Phi) = (q - U(T), \Phi(T))_Q, \\ 0 &= J'_q(q; U(T))(\delta q) + F'_q(q; Z)(\delta q) = (q - U(T), \delta q)_Q + (\delta q, Z(0)) \end{aligned}$$

for any $\Phi \in W$ and $\delta q \in Q$. In particular, the last formula gives a representation for the gradient of the minimization problem

$$\min_{q \in Q} j(q) := J(q, U_q(T))$$

where $U_q \in W$ denotes the unique solution of (7) for the given value $q \in Q$. More precisely, for given $q \in Q$ one can calculate the Q-gradient $\nabla j(q) \in Q$ as solution of

$$(\nabla j(q), \delta q)_Q = (q - U(T), \delta q)_Q + (\delta q, Z(0)) \tag{8}$$

for all $\delta q \in Q$, where Z and U are given as solutions to the first two equations of the optimality system. Notice, that for $\|(v, u)\|_Q := \int_\Omega v^2 + u^2 \mathrm{d}x$ this means

$$\nabla j(q) = q - U(T) + Z(0),$$

while for $\|(v, u)\|_Q := \int_\Omega v^2 + |\nabla u|^2 \mathrm{d}x$ the calculation of the gradient requires the solution of a PDE for the q_u component.

The above observation allows to formulate a standard gradient-descent method

Algorithm 7 (Gradient method) *Let $q^0 \in Q$ be an initial guess, and pick parameters $\gamma \in (0, 1/2)$ and $\alpha \in (0, 1)$. For $n = 1, 2, \ldots$ until $\|\nabla j(q^n)\|_Q < TOL$ iterate*

1. *Solve the primal problem*
$$B(U^n, \Phi) = F(q^{n-1}; \Phi).$$
2. *Solve the adjoint problem*
$$B(\Phi, Z^n) = J'_U(q^{n-1}; U^n(T))(\phi).$$
3. *Compute the gradient $\nabla j(q^{n-1})$ using (8).*
4. *Find the largest $k \in \{0, 1, \ldots\}$ such that (Armijo-rule)*
$$j(q^{n-1} - \alpha^k \nabla j(q^{n-1})) \le j(q^{n-1}) - \gamma \alpha^k \|\nabla j(q^{n-1})\|^2$$
holds and set $\alpha_n = \alpha^k$.
5. *Update*
$$q^n = q^{n-1} - \alpha_n \nabla j(q^{n-1}).$$

Similarly, we can construct an inexact Newton-type method, where the Newton equation

$$H(q)\delta q = -\nabla j(q)$$

is solved inexactly using a matrix-free CG-method. Here H denotes the Hessian operator $H(q) \colon Q \to Q$ of the reduced functional $j(q)$. For each subiteration of the CG-method requires the solution of two linear PDEs (the tangent and 'dual-for-hessian' equation), see, e.g., [3].

4.1 Discrete Setting

To simplify the notation, we discretize the time interval $I = (0, T)$ into discrete time steps of uniform size

$$0 = t_0 < t_1 < \cdots < t_M = T, \quad k := t_n - t_{n-1}. \tag{9}$$

We discretize in time with the backward Euler scheme. This can be interpreted as an approximation of the temporal Galerkin discretization with piecewise constant and discontinuous trial- and test-spaces on the subdivision (9), see [3, 4] for extensions to other time stepping schemes like variants of the Crank-Nicolson scheme and the necessary modifications required for dynamic time step sizes.

In the following, we give details on the discrete formulation for the strongly damped wave equation, written as first order system in $U = (v, u) \in W$ where $v = \partial_t u$. By $U_l = (v_l, u_l)$, we denote the approximation at time t_l. The control is given as $q = (q_v, q_u) \in Q$. The test function is denoted by Φ_k with $\Phi_l = (\phi_l, \psi_l)$ at time t_l. We introduce the discrete bilinear form $B_k(\cdot, \cdot)$ and the right hand sides of primal and dual problem

$$\begin{aligned} B_k(U_k, \Phi_k) &= \sum_{l=1}^{M} \Big\{ (v_l - v_{l-1}, \phi_l) + k\mu(\nabla u_l, \nabla \phi_l) + k\lambda(\nabla v_l, \nabla \phi_l) \\ &\qquad + (u_l - u_{l-1} - k v_l, \psi_l) \Big\} + (v_0, \phi_0) + (u_0, \psi_0), \\ F_k(q; \Phi_k) &= \sum_{l=1}^{M} k(f(t_l), \phi_l) + (q_v, \phi_0) + (q_u, \psi_0), \\ J_k(q, U_k; \Phi_k) &= \frac{1}{2}\Big((v_M - q_v, \phi_k) + (\nabla(u_M - q_u), \nabla \psi_l) \Big) \end{aligned} \tag{10}$$

where $F_l = F(t_l)$. Apart from the approximation of this right hand side (by the box rule), the backward Euler scheme corresponds to the dG(0) Galerkin discretization, compare to (6).

For spatial discretization, we employ a conforming finite element Galerkin scheme with $V_h \subset V$. For simplicity, we assume that V_h does not change over time. Extensions to dynamic meshes are described in the literature [4]. To keep the notation simple, we use $U_l \in V_h \times V_h$ to also denote the fully discrete approximation and skip the index 'h' referring to the spatial discretization. The control space is discretized by $V_h \times V_h \subset Q$. Given $U_0 := q = (q_v, q_u) \in V_h \times V_h$, we iterate for $l = 1, 2, \ldots, M$ to define the primal solution

$$\begin{aligned} (v_l, \phi_l) + k\mu(\nabla u_l, \nabla \phi_l) + k\lambda(\nabla v_l, \nabla \phi_l) &= (v_{l-1}, \phi_l) + k(f_l, \phi_l) \\ (u_l, \psi_l) - k(v_l, \psi_l) &= (u_{l-1}, \psi_l) \end{aligned} \tag{11}$$

The discrete adjoint problem is defined by swapping the role of trial- and test-function in (10) and $Z_k = (z_k, w_k) \in V_h \times V_h$ is defined as backward in time iteration of

$$\begin{aligned} (z_M, \phi_M) + k\lambda(\nabla z_M, \nabla \phi_M) - k(w_M, \phi_M) &= (v_M - q_v, \phi_M) \\ (w_M, \psi_M) + k\mu(\nabla z_M, \nabla \psi_M) &= (\nabla(u_M - q_u), \nabla \psi_M) \end{aligned}$$

$$\begin{aligned} (z_l, \phi_l) + k\lambda(\nabla z_l, \nabla \phi_l) - k(w_l, \phi_l) &= (z_{l+1}, \phi_l) \\ (w_l, \psi_l) + k\mu(\nabla z_l, \nabla \psi_l) &= (w_{l+1}, \psi_l) \end{aligned} \tag{12}$$

$$\begin{aligned} (z_0, \phi_0) &= (z_1, \phi_0) \\ (w_0, \psi_0) &= (w_1, \psi_0), \end{aligned}$$

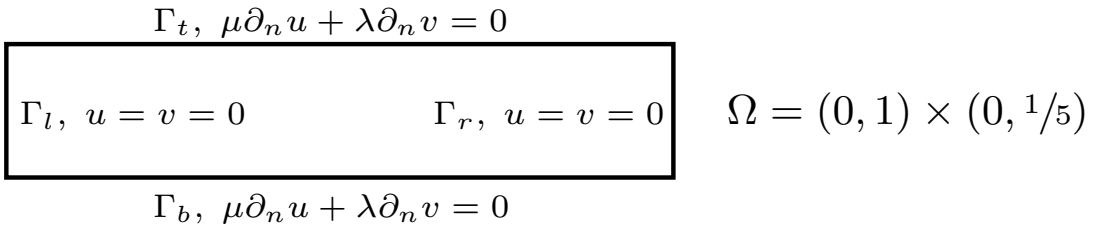

Figure 1: Configuration of the numerical test-cases. Domain of size width 1 and height 0.2. Free boundaries on the bottom and the top, homogeneous Dirichlet values on the left and the right.

where first and last steps differ from the intermediate ones.

This setting can be extended to higher order time-discretizations like the Crank-Nicolson scheme as variant of a temporal Galerkin scheme with piecewise linear continuous trial functions and piecewise constant discontinuous test-functions or to variants with better stability like the shifted θ-time stepping scheme or the fractional step theta scheme [11, 20]. Furthermore it is possible to incorporate dynamic meshes [19] and non-uniform time steps. An extension to nonlinear problems (like the Navier-Stokes equations) is described in [4].

5 Numerical tests

In this part, we discuss two numerical test cases following the abstract setting and the discretization introduced in the previous sections. First, we consider the damped wave equation with an oscillatory right hand side. Second, we introduce an additional nonlinearity. Both problems are given on a rectangular domain of size 1×0.2, see figure 1. On the left and the right, we prescribe homogeneous Dirichlet values for u and v, on the upper and lower boundary the solution is free, i.e.,

$$u = v = 0 \text{ on } \Gamma_{\mathrm{l/r}}, \quad \mu\partial_n u + \lambda\partial_n v = 0 \text{ on } \Gamma_{t/b}.$$

The problem is driven by the oscillatory right hand side (spatially constant)

$$f(t) = \sin(2\pi t) + \frac{1}{10}\cos(14\pi t). \tag{13}$$

It holds $f(t) = f(t+T)$ for $T = 1$. In all numerical test cases, we use piecewise bilinear elements on a quadrilateral mesh with 1 024 elements and the uniform time step size $k = 0.01$.

In Section 3, we equipped Q with the norm $L^2(\Omega) \times H^1(\Omega)$, see (4). The numerical test-cases are mostly performed using the norm

$$\|q\|_Q^2 = \|q_v\|^2 + \|q_u\|^2,$$

for which we cannot show the smoothing property required to satisfy Assumption 1. This norm however allows for a more efficient numerics, since (8) can be solved trivially. We will add one numerical test case that highlights the use of the correct norm $L^2 \times H^1$.

5.1 Linear damped wave equation problem

We consider the wave equation written as first order system in time

$$\begin{aligned} \partial_t v - \mu\Delta u - \lambda\Delta v &= f(t) \\ \partial_t u - v &= 0, \end{aligned}$$

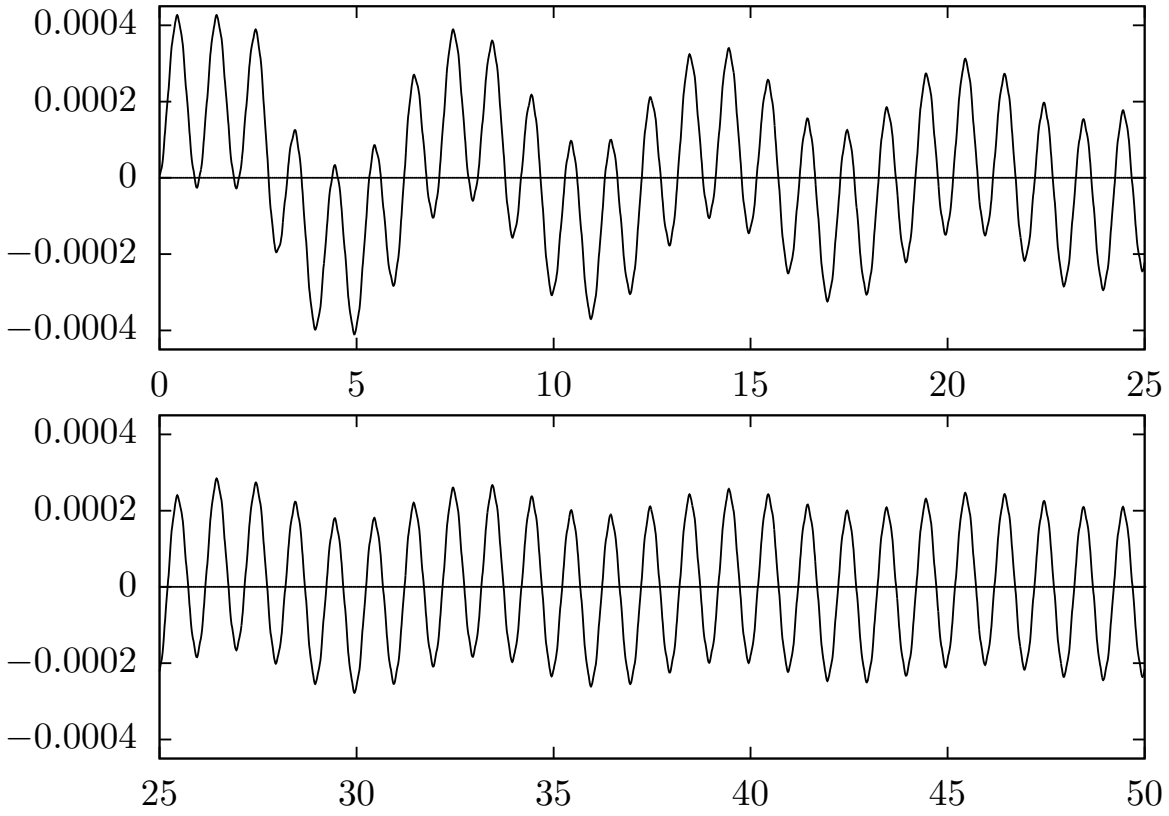

Figure 2: The functional $N(U(t))$ measuring the stress on the left and right boundaries plotted over the first 50 cycles.

with a periodic right hand side specified in (13) and the parameters

$$\mu = 0.1, \quad \lambda = 0.01$$

In Figure 2, we plot the functional

$$N\left(U(t)\right) = \int_{\Gamma_l \cup \Gamma_r} \left(\mu \partial_n u(t) + \lambda \partial_n v(t)\right) \, \mathrm{d}s$$

as function over time in for the first 50 periods, the interval $[0, 50]$. As initial solution at time $t = 0$, we used $q_v = q_u = 0$. The derivation from the periodic state is still easily visible after all 50 cycles.

Next, we directly identify the optimal initial data $q = (q_v, q_u)$ by means of the gradient method and the Newton scheme. We start the optimization routines with the initial guess $q_v = q_u = 0$. In Figure 3, we indicate the reduction of the functional

$$J(q; U_N) = \frac{1}{2}\|v_N - q_v\|^2 + \frac{1}{2}\|u_N - q_u\|^2$$

compared to the initial error in periodicity. The left sketch in the figure shows the reduction of $J(\cdot)$ plotted over the necessary outer iterations for gradient- and Newton-scheme. We see an enormous benefit of the optimization approaches. Further, the Newton scheme shows quadratic convergence. In the right sketch we plot the functional error over the required number of cycles, i.e., PDE solutions,

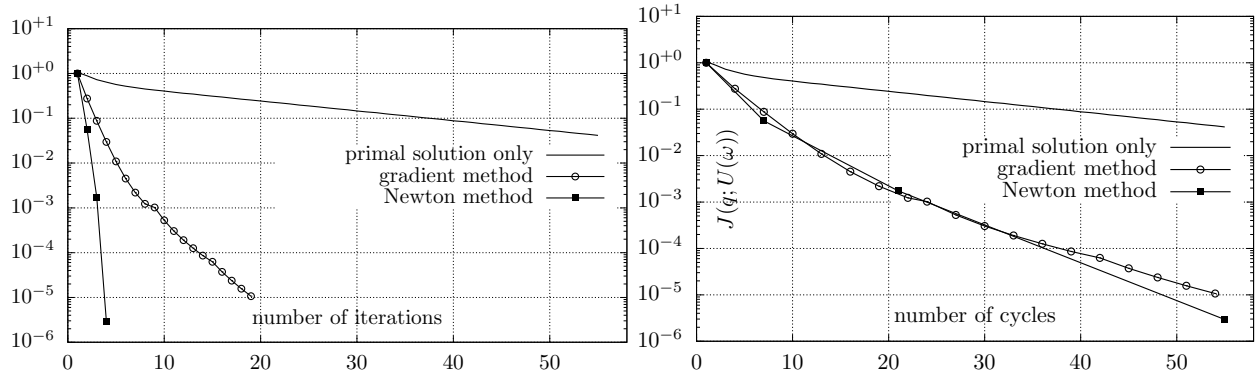

Figure 3: Relative reduction of the function $J(q;U)$ for the solution of the primal problem. In the left figure we show the convergence in terms of iterations of forward solution, gradient scheme and Newton scheme. In the right figure we show the reduction measured in solution cycles including all primal and adjoint solves.

necessary to run both the Newton- and the gradient-scheme. This includes all primal forward simulations, the adjoint solves of the gradient scheme, and the tangent equations required in the Newton scheme. Compared to the forward simulation, we still have a substantial improvement in terms of computational complexity. Although the number of Newton iterations is much less than the number of gradient iterations we do not benefit as significantly in terms of computational effort.

To compare the efficiency of the gradient scheme with a direct forward solution running into the periodic solution, we plot the functional values over the number of cycles (PDE solutions over a time interval of length T) required. In the case of the forward solution, we count all cycles of length $T = 1$; for the gradient scheme, we count all cycles of the forward and the adjoint problem, both in steps 1. and 2. of Algorithm 7 and further necessary cycles within the Armijo rule in step 4. of the algorithm. For the Newton scheme, we also count all steps required for the inexact step calculation as well as the line search. This counting allows for a fair comparison of the computational effort in case of a linear PDE, since all PDE solutions are approximately of equal cost. Considering the gradient scheme and the Newton scheme, we plot the functional values $J(q^{n-1};U_N^n)$ in the case of the forward problem, we plot $J(U(t_n - T);U(t_n))$ as a measure of periodicity.

While the simple forward simulation reduced the error by only on order of magnitude within the first 50 cycles, both optimization strategies yield a reduction of more then 5 orders in the same total number cycles. We note that the Newton scheme arrives at this low residual in only three steps.

Next, in Figure 4, we show the same comparison of the three different approaches (direct forward simulation, gradient and Newton method) using the $L^2(\Omega)\times H^1(\Omega)$-norm in J that allows us to comply with Assumption 1 according to Theorem 6. Here, we see a greater benefit of using the Newton scheme as compared to the gradient method. Again, both optimization approaches by far outrun the simple forward computation.

5.2 Convergence in space and time

To analyze the robustness of the optimization scheme with respect to spatial and temporal discretization, we add further computational results on sequences of temporal and spatial meshes. For measuring

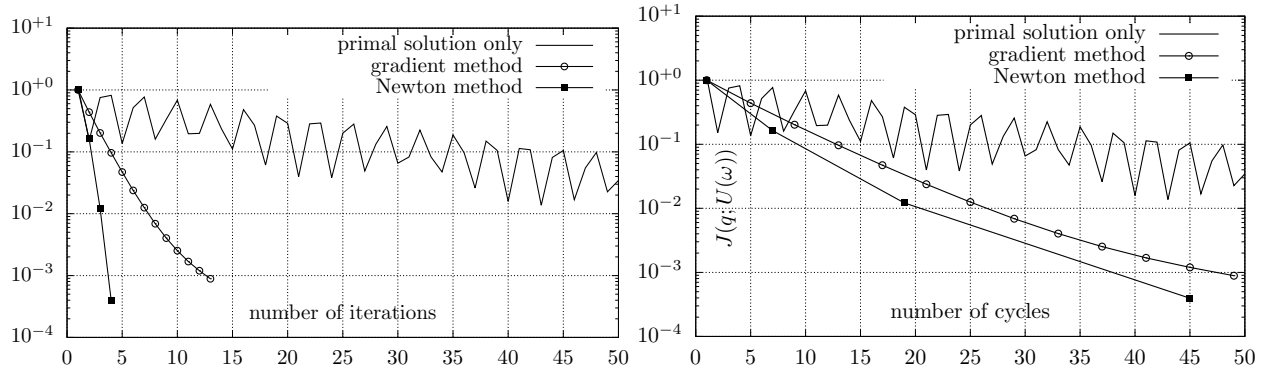

Figure 4: Reduction of the function $J(q;U)$ for the solution of the primal problem measured after every cycle and for the gradient method. In contrast to Figure 3, we now use the correct norm $L^2(\Omega) \times H^1(\Omega)$ for defining the goal functional.

the discretization error we introduce the goal functional

$$J(U) = \int_I \int_\Omega |v| \, \mathrm{d}x \, \mathrm{d}t. \tag{14}$$

An accurate reference value J_{ref} is obtained on fine spatial and temporal meshes

$$J_{\mathrm{ref}} = 0.02080.$$

In Figure 5, we show the error in the functional (14) under refinement of the spatial and temporal discretization, i.e. $|J(u) - J(u_{kh})|$. For comparison, we give results for methods of first and second order; like in the previous section, we use the dG(0) Galerkin discretization in time with piecewise bilinear finite elements in space and, in addition, we give results obtained with the cG(1) Galerkin discretization in time (that corresponds to the trapezoidal rule) combined with piecewise biquadratic finite elements in space. The initial meshes each contain 162 spatial degrees of freedom and the temporal interval is split into 25 time steps. Refinement is uniform in space and time such that $h \sim k$. Both methods show the expected linear and quadratic order of convergence.

Figure 6 shows the Newton convergence for reducing the periodicity error in the functional $J(q;U_N)$. The Newton scheme is very robust with respect to refinement of temporal and spatial meshes. When using quadratic discretizations in space and time one additional Newton step is required to reach the desired tolerance in the periodicity error.

5.3 Nonlinear Problem

As a second test case, we introduce a nonlinearity and solve

$$\begin{aligned} \partial_t v - \mu \Delta u - \lambda \Delta v + u^2 v &= f(t), \\ \partial_t u - v &= 0. \end{aligned}$$

This equation does not fit into the theoretical framework used in Section 2, as we only considered linear problems. Nevertheless, we add a nonlinear test case to demonstrate the feasibility of the optimization approach as a computational tool for accelerating the search for periodic solutions. We consider the same oscillatory forcing term $f(t)$ with periodicity $T = 1$ and stick to the parameters

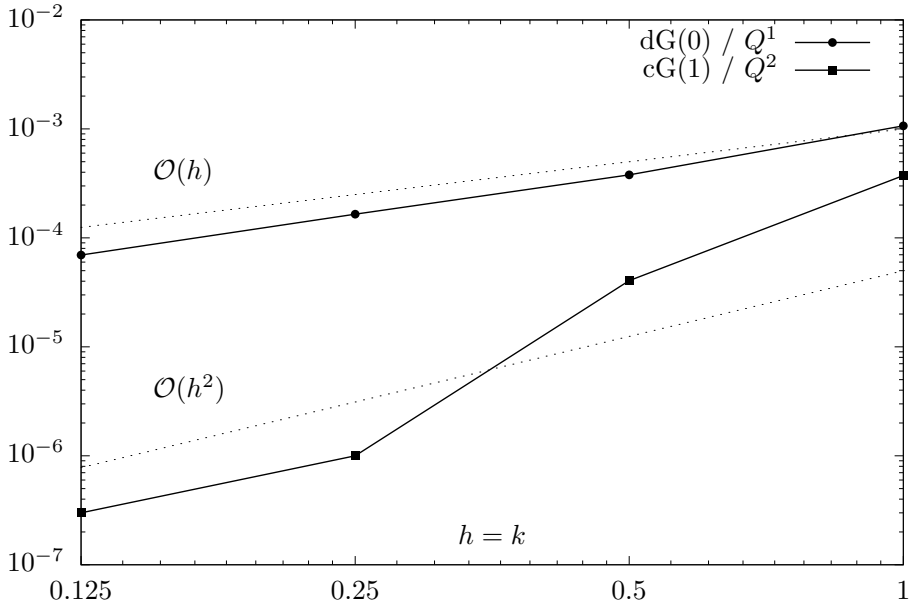

Figure 5: Convergence of the discretization error $|J(u) - J(u_{kh})|$ for first order and second order discretizations under uniform refinement of the spatial and temporal mesh. The coarsest mesh level corresponds to 162 spatial degrees of freedom (for Q^1 and Q^2) and 25 time steps.

$\mu = 0.1$, $\lambda = 0.01$. The boundary data is set as for the linear case. Again, we start by the plotting the functional

$$N\left(U(t)\right) = \int_{\Gamma_l \cup \Gamma_r} \left(\mu \partial_n u(t) + \lambda \partial_n v(t)\right) \, \mathrm{d}s$$

as function of time, see Figure 7, where we show the interval $[0, 50]$. The structure of the solution is similar to the linear test case. The fundamental difference between linear and nonlinear problems is given in the computational effort. While the primal problem might be linear, the dual problem is always a linear problem with potentially lower computational cost.

Finally, in Figure 8, we give a comparison of the forward solution with the gradient method and the Newton scheme. Like in the linear case, we consider the simplified functional based on the $L^2(\Omega)$-norm

$$J(q; U_N) = \frac{1}{2}\|v_N - q_v\|^2 + \frac{1}{2}\|u_N - q_u\|^2.$$

We compare the reduction in $J(\cdot)$ over the number of required solution cycled relative to the initial value. Again, we observe a significant decrease in computational effort by using a systematic optimization approach in running to the cyclic state. The Newton scheme again shows quadratic convergence to the periodic solution. In about 60 cycles, gradient and Newton scheme are able to reduce the goal functional by more than 3 orders of magnitude compared to a reduction between 1 and 2 orders of magnitude obtained with the simple forward simulation.

In contrast to the linear case, the Newton method is a bit more favorable here, since nonlinear PDEs need to be solved only once in each iteration and eventually during line search - which here only occurred for the gradient method.

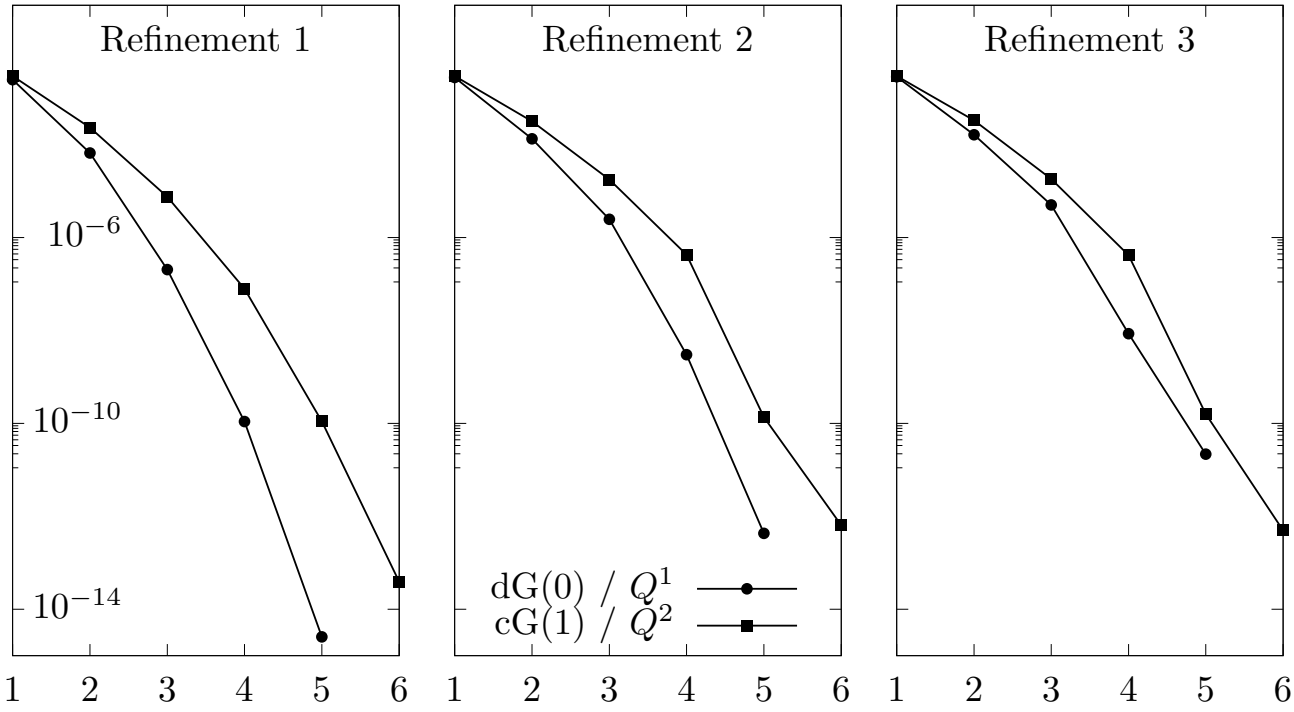

Figure 6: Convergence of the Newton scheme for reducing the periodicity error under refinement of the spatial and temporal mesh. The second order scheme based on cG(1) time stepping and biquadratic elements requires one additional Newton step.

6 Conclusion

We have introduced a new numerical approach for the efficient simulation of cyclic states with partial differential equations. In contrast to space-time techniques or approaches based on the shooting method, we only require the simulation of standard primal and dual solutions. There are various possibilities for enhancing the efficiency of the proposed scheme:

- The optimization loops can be run in a hierarchical configuration similar to [18] using coarse temporal and spatial meshes. This approach is promising as the dual solutions that are already available can be used to guide adaptive schemes for a control of optimization error in $q - u_N$ as well as spatial and temporal discretization error.

- The Newton scheme is highly effective in terms of Newton iterations. For both problems the desired residual of 10^{-8} is reached in only three steps. Still a large number of linear PDE solutions is required within to find a good line search parameter.

- With dG(0) and cG(1) Galerkin discretization and piece-wise bilinear or biquadratic finite elements, we have schemes of relatively low order. The testcase in Section 5.2 has shown very little sensitivity of the optimization approach to the chosen discretization methods. The extension to higher order spatial discretization is straightforward. Concerning the temporal discretization higher order Galerkin schemes have already been successfully applied to gradient based optimization [24, 23] and can be embedded in our context.

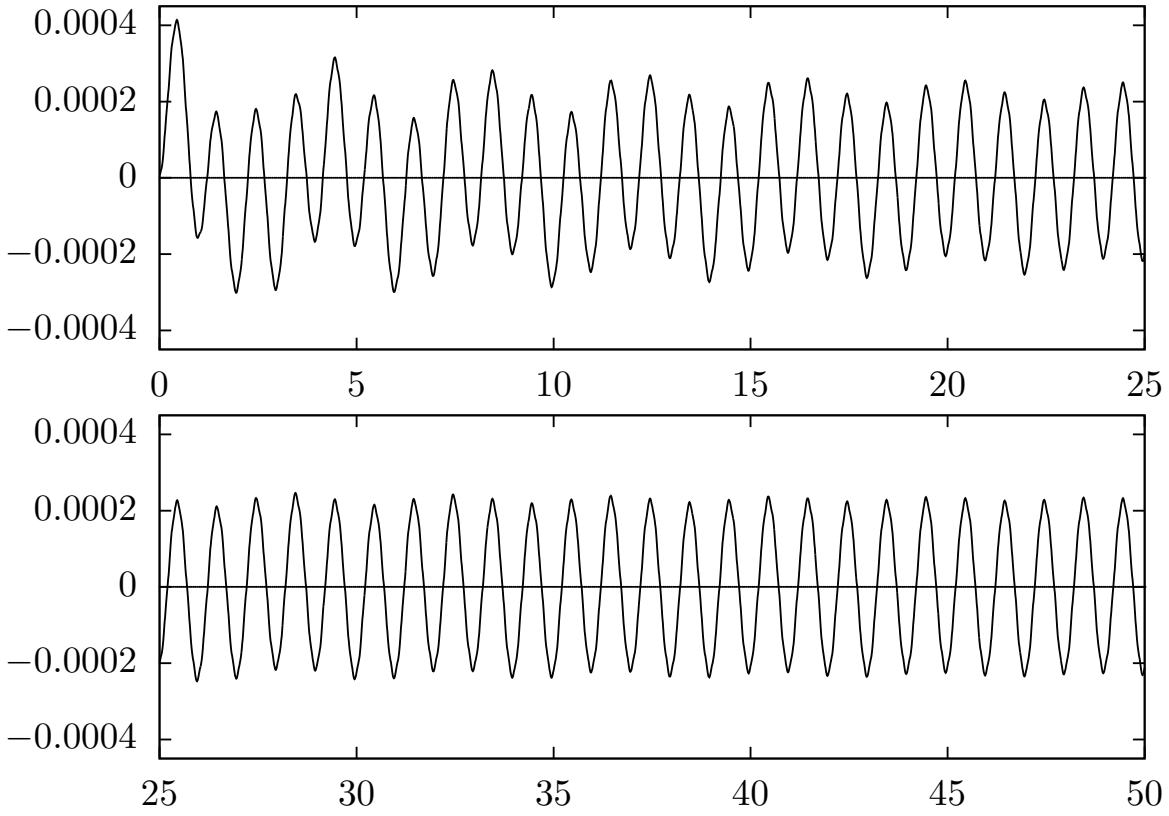

Figure 7: First 50 cycles of the nonlinear test case. Showing the functional $N(U(t))$.

A next step is the application of the optimization schemes to problems where the periodicity T is not known a priori. Such situations frequently appear in fluid dynamics regarding the self-excited oscillatory flow around obstacles. The interval length T must be added as unknowns to the optimization problem, e.g.,

$$J(q, T; U) := \frac{1}{2}\|q - U(T)\|^2 \quad \mapsto \quad \min .$$

References

[1] Ambrose, D.M., Wilkening, J.: Computation of time-periodic solutions of the Benjamin-Ono equation. J. Nonlinear Sci. **20**(3), 277–308 (2010). DOI 10.1007/s00332-009-9058-x

[2] Ang, D.D., Dinh, A.P.N.: On the strongly damped wave equation: $u_{tt} - \Delta u - \Delta u_t + f(u) = 0$. SIAM J. Math. Anal. **19**(6), 1409–1418 (1988). DOI 10.1137/0519103

[3] Becker, R., Meidner, D., Vexler, B.: Efficient numerical solution of parabolic optimization problems by finite element methods. Optim. Methods Softw. **22**(5), 813–833 (2007). DOI 10.1080/10556780701228532

[4] Besier, M., Rannacher, R.: Goal-oriented space-time adaptivity in the finite element galerkin method for the computation of nonstationary incompressible flow. Internat. J. Numer. Methods Fluids **70**(9), 1139–1166 (2012). DOI 10.1002/fld.2735

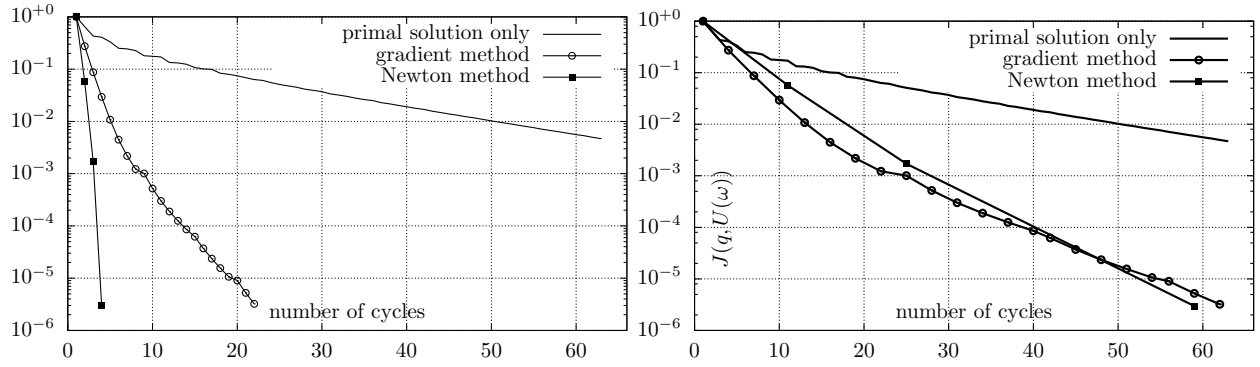

Figure 8: Reduction of in the function $J(q;U)$ for the solution of the primal problem measured after every cycle and for the gradient method. The left sketch shows the reduction over the number of iterations, the right sketch gives the reduction depending on the overall number of cycles that have been computed. For the gradient method this is the sum of primal and adjoint cycles.

[5] Bock, H.G.: Randwertproblemmethoden zur Parameteridentifizierung in Systemen nichtlineare Differentialgleichungen, *Bonner Mathematische Schriften*, vol. 183. Universität Bonn, Mathematisches Institut, Bonn (1987)

[6] Chakraborty, P., Ghosh, S.: Accelerating cyclic plasticity simulations using an adaptive wavelet transformation based multitime scaling method. Internat. J. Numer. Methods Engrg. **93**, 1425–1454 (2013). DOI 10.1002/nme.4459

[7] Crouch, R., Oskay, C.: Accelerated time integrator for multiple time scale homogenization. Internat. J. Numer. Methods Engrg. **101**, 1019–1042 (2015). DOI 10.1002/nme.4863

[8] Frei, S., Richter, T., Wick, T.: Long-term simulation of large deformation, mechano-chemical fluid-structure interactions in ale and fully eulerian coordinates. J. Comput. Phys. **321**, 874–891 (2016). DOI 10.1016/j.jcp.2016.06.015

[9] Galdi, G.P.: On bifurcating time-periodic flow of a navier-stokes liquid past a cylinder. Arch. Rational Mech. Anal. **222**(1), 285–315 (2016). DOI 10.1007/s00205-016-1001-3

[10] Galdi, G.P., Kyed, M.: Time-periodic solutions to the navier-stokes equations in three-dimensional whole-space with a non-zero drift term: Asymptotic profile at spatial infinity (2016). URL arXiv:1610.00677v1

[11] Goll, C., Rannacher, R., Wollner, W.: On the adjoint to the damped Crank-Nicolson time marching scheme: Applications to goal-oriented mesh adaptation for the Black-Scholes equation. J. Comput. Finance **18**(4), 1–37 (2015). DOI 10.21314/JCF.2015.301

[12] Govindjee, S., Potter, T., Wilkening, J.: Cyclic steady states of treaded rolling bodies. Int. J. Num. Meth. Engrg. **99**, 203–220 (2014)

[13] Hante, F., Mommer, M., Potschka, A.: Newton-picard preconditioners for time-periodic parabolic optimal control problems. SIAM J. Numer. Anal. **53**(5), 2206–2225 (2015)

[14] Hinze, M., Pinnau, R., Ulbrich, M., Ulbrich, S.: Optimization with PDE Constraints, *Mathematical Modelling: Theory and Applications*, vol. 23. Springer (2009)

[15] Jiang, L., Biegler, L.T., Fox, V.G.: Simulation and optimization of pressure-swing adsorption systems for air separation. AIChE Journal **49**(5), 1140–1157 (2003). DOI 10.1002/aic.690490508

[16] Kato, H.: Existence of periodic solutions of the Navier-Stokes equations. J. Math. Anal. Appl. **208**(1), 141–157 (1997). DOI https://doi.org/10.1006/jmaa.1997.5307

[17] Lions, J.L.: Optimal Control of Systems Governed by Partial Differential Equations, 1. edn. Die Grundlehren der mathematischen Wissenschaften. Springer, Berlin – Heidelberg – New York (1971)

[18] Lübke, R., Seidel-Morgenstern, A., Tobiska, L.: Numerical method for accelerated calculation of cyclic steady state of ModiConSMB-processes. Computers & Chemical Engineering **31**(4), 258–267 (2007). DOI 10.1016/j.compchemeng.2006.06.013

[19] Meidner, D.: Adaptive space-time finite element methods for optimization problems governed by nonlinear parabolic systems. Ph.D. thesis, University of Heidelberg (2008)

[20] Meidner, D., Richter, T.: Goal-oriented error estimation for the fractional step theta scheme. Comput. Methods Appl. Math. **14**, 203–230 (2014). DOI 10.1515/cmam-2014-0002

[21] Pao, C.V.: Numerical methods for time-periodic solutions of nonlinear parabolic boundary value problems. SIAM J. Numer. Anal. **39**(2), 647–667 (2001). DOI 10.1137/S0036142999361396

[22] Platte, F., Kuzmin, D., Fredebeul, C., Turek, S.: Novel simulation approaches for cyclic-steady-state fixed-bed processes exhibiting sharp fronts and shocks. In: M. de Bruin, D. Mache, J. Szabados (eds.) Trends and applications in constructive approximations, *International series of numerical mathematics*, vol. 151, pp. 207–233. Birkhäuser (2005). DOI 10.1007/3-7643-7356-3_15

[23] Springer, A.: Efficient higher order discontinuous galerkin time discretizations for parabolic optimal control problems. Ph.D. thesis, Technische Universität München (2015). Urn:nbn:de:bvb:91-diss-20150519-1237294-1-6

[24] Springer, A., Vexler, B.: Third order convergent time discretization for parabolic optimal control problems with control constraints. Computational Optimization and Applications **57**(1), 205–240 (2014)

[25] Steuerwalt, M.: The existence, computation, and number of solutions of periodic parabolic problems. SIAM J. Numer. Anal. **16**(3), 402–420 (1979). DOI 10.1137/0716034

[26] Toumi, A., Engell, S., Diehl, M., Bock, H.G., Schlöder, J.: Efficient optimization of simulated moving bed processes. Chemical Engineering and Processing: Process Intensification **46**(11), 1067–1084 (2007). DOI 10.1016/j.cep.2006.06.026

[27] Tröltzsch, F.: Optimal control of partial differential equations, *Graduate Studies in Mathematics*, vol. 112. American Mathematical Society, Providence, RI (2010)

[28] Webb, G.F.: Existence and asymptotic behavior for a strongly damped nonlinear wave equation. Canad. J. Math. **32**(3), 631–643 (1980). DOI 10.4153/CJM-1980-049-5

[29] Wloka, J.: Partial Differential Equations. Cambridge University Press (1987)

[30] Yang, Y., Jaeger, W., Neuss-Radu, M., Richter, T.: Mathematical modeling and simulation of the evolution of plaques in blood vessels. J. Math. Biol. **72**, 973–996 (2016). DOI 10.1007/s00285-015-0934-8

[31] Yang, Y., Richter, T., Jaeger, W., Neuss-Radu, M.: An ale approach to mechano-chemical processes in fluid-structure interactions. Internat J. Numer. Methods Fluids **84**(4), 199–220 (2017). DOI 10.1002/fld.4345

[32] Zahr, M.J., Persson, P.O., Wilkening, J.: A fully discrete adjoint method for optimization of flow problems on deforming domains with time-periodicity constraints. Computers and Fluids **139**, 130–147 (2016)

[33] Zuyev, A., Seidel-Morgenstern, A., Benner, P.: An isoperimetric optimal control problem for a non-isothermal chemical reactor with periodic inputs. Chemical Engineering Science **161**, 206–214 (2016). DOI 10.1016/j.ces.2016.12.025